Journal of Hazardous Materials 438 (2022) 129470

Contents lists available at ScienceDirect

Journal of Hazardous Materials

journal homepage: www.elsevier.com/locate/jhazmat

Research Paper

Long-term exposure to nanoplastics alters molecular and functional traits related to the carcinogenic process

Irene Barguilla [a], Josefa Domenech [a], Sandra Ballesteros [a], Laura Rubio [b], Ricard Marcos [a,*], Alba Hernández [a,*]

[a] Group of Mutagenesis, Department of Genetics and Microbiology, Faculty of Biosciences, Universitat Autònoma de Barcelona, Cerdanyola del Vallès, Barcelona, Spain
[b] Nanobiology Laboratory, Department of Natural and Exact Sciences, Pontificia Universidad Católica Madre y Maestra, PUCMM, Santiago de los Caballeros, Dominican Republic

HIGHLIGHTS

- The carcinogenic risk of polystyrene nanoplastics (PSNPLs) was evaluated.
- Long-term exposures (6 months) were used.
- A sensitive cell model showing cell-transforming phenotype was used.
- PSNPLs exposure exacerbated most of the evaluated hallmarks of cancer.
- This data constitutes a relevant warning on the potential carcinogenic risk of MNPLs.

GRAPHICAL ABSTRACT

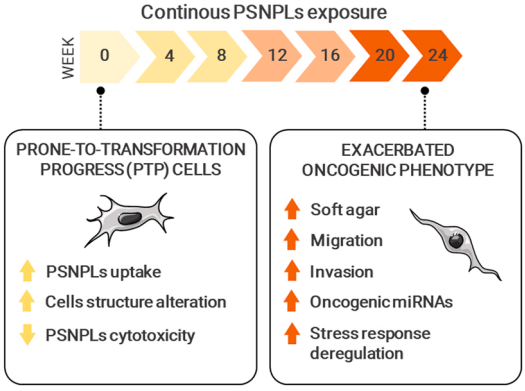

ARTICLE INFO

Editor: Youn-Joo An

Keywords:
Polystyrene nanoplastic
Long-term exposure
Cell transformation
Oncogenic phenotype
Carcinogenesis

ABSTRACT

Micro/nanoplastics (MNPLs) are considered emergent pollutants widely spread over all environmental compartments. Although their potential biological effects are being intensively evaluated, many doubts remain about their potential health effects in humans. One of the most underdeveloped fields is the determination of the potential tumorigenic risk of MNPLs exposure. To shed light on this topic, we have designed a wide battery of different hallmarks of cancer applied to prone-to-transformed progress MEF cells exposed to polystyrene nanoplastics (PSNPLs) in the long term (6 months). Interestingly, most of the evaluated hallmarks of cancer are exacerbated after exposure, independently if they are associated with an early tumoral phenotype (changes in stress-related genes, or microRNA deregulation), advanced tumoral phenotype (growing independently of anchorage ability, and migration capacity), or an aggressive tumoral phenotype (invasion potential, changes in

* Corresponding authors at: Group of Mutagenesis, Department of Genetics and Microbiology, Faculty of Biosciences, Universitat Autònoma de Barcelona, Cerdanyola del Vallès, Barcelona, Spain.
E-mail addresses: ricard.marcos@uab.es (R. Marcos), alba.hernandez@uab.es (A. Hernández).

https://doi.org/10.1016/j.jhazmat.2022.129470
Received 25 January 2022; Received in revised form 8 June 2022; Accepted 24 June 2022
Available online 27 June 2022

pluripotency markers, and ability to grow to form tumorspheres). This set of obtained data constitutes a relevant warning on the potential carcinogenic risk associated with long-term exposures to MNPLs, specifically that induced by the PSNPLs evaluated in this study.

1. Introduction

One of the most worrisome aspects of the widespread micro- and nanoplastic (MNPLs) pollution is the potential health effects triggered by their long-term exposure. Secondary MNPLs, generated from the environmental degradation of macroplastic waste, are present everywhere and, consequently, humans are continuously exposed to them by different routes including ingestion, inhalation, and dermal deposition (Bouwmeester et al., 2015; Domenech and Marcos, 2021). Therefore, risk assessment approaches evaluating the potential long-term effects of MNPLs exposure are urgently required (Brachner et al., 2020).

Up to date, several studies have found detrimental biological effects associated with MNPLs exposure, mostly following acute regimes. Using *in vitro* approaches different authors have described the ability of MNPLs to efficiently internalize in diverse cell lines, and translocate through physiological barriers (Hesler et al., 2019; Domenech et al., 2020), inducing reactive oxygen species (ROS) formation (Schirinzi et al., 2017), DNA damage (Rubio et al., 2020a), inflammation (Ballesteros et al., 2020; Hu and Palić, 2020), mitochondrial dysfunction, stress, and autophagy (Wang et al., 2021). However, very few studies explore these -or other- endpoints in a chronic exposure context, which would be more representative of a real-life exposure scenario. Among those studies found in the literature, the work by Domenech et al. (2021) showed that Caco-2 cells exposed to low-range doses of polystyrene nanoplastic (PSNPLs) altered the expression levels of stress-related genes such as *HO1* and *SOD2*. However, no other pieces of evidence of ROS induction, genotoxicity, or oxidative DNA damage were observed, despite the constant intake of PSNPLs by the cells, and the observed structural changes associated with its accumulation. The impact of the sub-chronic exposure to MNPLs has also been explored after a 48-day exposure of HT-29 cells to polystyrene microplastics (PSMPLs). Thus, Visalli et al. (2021) showed that ROS and DNA damage induction by short-term exposures to PSMPLs were less evident under sub-chronic exposure settings, hinting at the adaptability of the intestinal cells to PSMPLs exposure. Taken together, these results prove that differential and accumulative effects are induced depending on the exposure settings.

It is important to point out the critical lack of information on carcinogenicity-related endpoints associated with MNPLs exposure. It should be considered that carcinogenic effects are potential hazards associated with environmental long-term exposures. Therefore, in this study, we aimed to propose/use a battery of *in vitro* carcinogenesis biomarkers, including stress-response deregulation, microRNA expression alteration, invasive potential, and cell dedifferentiation associated with long-term MNPLs exposure. These transformation markers are descriptive of specific features acquired by transformed cells during the oncogenic process and align with relevant hallmarks of carcinogenesis, such as the cells' invasive potential (Hanahan and Weinberg, 2011). To assess these carcinogenic-related endpoints, we have chosen a pre-transformed cell model of mouse embryonic cells (MEFs), sensitive to oxidative damage induction. In our long-term experiment, such model cells were exposed to PSNPLs for 6 months. As indicated, the selected cells already exhibited a characteristic tumor-associated phenotype as evidenced by their acquired spindle-like morphology, invasiveness potential, and altered differentiation status (Bach et al., 2016). Therefore, the sensitized genetic background of our cell model may facilitate the identification of mild effects that typically can be unnoticed in a normal cellular context. After characterizing the short-term dynamics of the nanoplastic uptake in our system, we explored both molecular and functional biomarkers of *in vitro* carcinogenesis at the end of the 6-month exposure period.

2. Materials and methods

2.1. PSNPs and y-PSNPs characterization

Pristine PSNPLs (PP-008–10) and yellow fluorophore-conjugated PSNPLs (y-PSNPLs) (FP-00552-2) were purchased from Spherotech (Chicago, USA). Pristine PSNPLs were used in all experimental work except for the quantification of PS nanoparticles internalization by flow cytometry, for which the fluorescently labeled particle was required. Nanoplastic characterization was performed using a Zetasizer device and transmission electron microscopy (TEM). For that purpose, the PSNPLs dispersions were diluted to a final concentration of 100 μg/mL in distilled water or in a culture medium (DMEM). The hydrodynamic size and Z-potential parameters were analyzed in triplicates with a Malvern Zetasizer Nano ZS zen3600 device (Malvern, UK), applying dynamic light scattering (DLS) and electrophoretic light scattering (ELS) approaches. On the other hand, carbon-coated TEM grids were dipped into the PSNPLs dispersions and visualized on a JEOL JEM-1400 instrument (JEOL LTD, Tokyo, Japan). To determine the mean particle size, 100 randomly selected PSNPLs were measured using Image J software with the Fiji extension.

2.2. Cell culture conditions

Mouse embryonic fibroblasts, phenotypically sensitive to oxidative damage (*Ogg1*$^{-/-}$), and initially transformed by 30 weeks of chronic sodium arsenite (As^{III}) exposure (2 μM) (Bach et al., 2016), were used. These cells are referenced from this point forward as prone-to-transformation progress (PTP) cells. PTP cells were grown in Dulbecco's modified Eagle's medium (DMEM)/F12 medium (Life Technologies, NY, USA) supplemented with 10 % fetal bovine serum (Biowest, France) and 2.5 μg/mL Plasmocin (InvivoGen, CA, USA) in a humidified atmosphere of 5 % CO_2 and 95 % air at 37 °C.

2.3. PSNPLs cytotoxicity

To assess the potential cytotoxicity associated with the exposure to PSNPLs in PTP cells, viability was determined by the Beckman counter method with a ZTM Series Coulter-counter (Beckman Coulter Inc., CA, US). Briefly, 24 h after seeding 80,000 cells on 12-well plates, cells were treated with increasing doses of PSNPLs (10, 25, 75, and 100 μg/mL). After exposures lasting for 24 h, the cells were counted and the percentages of viable cells with respect to the non-exposed control were represented.

2.4. PSNPLs internalization in PTP cells

The quantification of the PSNPLs internalization after acute exposure was carried out by flow cytometry. PTP cells were exposed to 25 μg/mL y-PSNPLs for 24, 48, or 72 h. Then, the cells were washed with PBS 1X, trypsinized, centrifuged, and resuspended in PBS 1X at a final concentration of 1×10^6 cells/mL. 200 μL of the cell suspension were transferred to a 96-well plate. Propidium iodide (1:1000) was added to discriminate alive cells within the total population. CytoFlex (Beckman Coulter Inc., CA, US) was used for the analysis. Approximately 10,000 events per sample out of the living population were analyzed. The PSNPLs internalization was extrapolated from the mean fluorescence intensity.

2.5. Intracellular PSNPLs detection

TEM was used to determine potential changes in the cellular structure induced by PSNPLs uptake. After a 24, 48, or 72 h exposure to 25 μg/mL PSNPLs, cells were washed with PBS 1X, trypsinized, pelleted, and fixed in 2.5 % (v/v) glutaraldehyde (EM grade, Merck, Darmstadt, Germany) and 2 % (w/v) paraformaldehyde (EMS, Hatfield, USA), in 0.1 M cacodylate buffer (PB, Sigma-Aldrich, Germany) at pH of 7.4. Then, sampling processing was carried out following conventional procedures, as previously reported (Annangi et al., 2015). A Jeol 1400 TEM (Jeol LTD, Tokyo, Japan) equipped with a CCD GATAN ES1000W Erlangshen camera was used to take representative cell images.

2.6. In vitro chronic PSNPLs exposure

PTP cells were chronically exposed for 6 months to 25 μg/mL PSNPLs. Replicates of exposed cells (PSNPLs) and non-exposed passage-matched controls (CT) were maintained in two separate T-25 flasks and grown under the culture conditions previously described. To ensure a constant exposure condition in the long-term exposure experiments, the cell culture medium was replaced every 2–3 days with new media containing the selected concentration of PSNPLs.

2.7. Total RNA extraction

Total RNA from control and PSNPLs-exposed PTP cells was extracted using TRI® Reagent (Sigma-Aldrich, Germany) and following the manufacturer's instructions. DNA contamination was removed using RNase-free DNase I (Turbo DNA-free Kit; Invitrogen, CA, USA).

2.8. mRNA retrotranscription and expression evaluation by Real-Time-qPCR

From total RNA, the first-strand cDNA synthesis was performed using 1 μg of total RNA and the high-capacity RNA-to-cDNA Kit (Applied Biosystems, CA, USA). Real-time PCR analysis on a LightCycler 480 was used to determine the relative expression of panels of stress-, EMT- or stemness-related genes, with *Actb* as the housekeeping control. Each 20 μL of reaction volume contained 5 μL of cDNA, 10 μL of 2 × LightCycler 480 SYBR Green I Master (Roche, Manheim, Germany), 3 μL of H_2O, and 1 μL of each primer pair at a final concentration of 500 nM. The cycling parameters began with 95 °C for 5 min, then 45 cycles of 95 °C for 10 s, 61 °C for 15 s, and 72 °C for 25 s. The target genes and their corresponding primer sequences are listed in the supplementary Table S1. The LightCycler software package was used to calculate cycle time values which were then normalized by the *Actb* data.

2.9. microRNA retrotranscription and expression evaluation by Real-Time-qPCR

Changes in the microRNAs' expression were evaluated by Real-Time RT-PCR. To proceed, a mix including 80 ng of total RNA, 1 μL of 10X poly(A) polymerase buffer, 10 mM of ATP, 1 μM of RT-primer (Sigma-Aldrich, Germany), 0.1 mM of each deoxynucleotide (dATP, dCTP, dGTP, and dTTP) (VWR International, Ireland), 100 units of MulV reverse transcriptase (New England Biolabs, USA), and 1 unit of Poly(A) polymerase (New England, Biolabs USA) was prepared at a final volume of 10 μL. The mix was incubated for 1 h at 37 ºC before to an enzyme activation step at 95 ºC for 5 min. The sequence of the RT-primer was 5′-CAGGTCCAGTTTTTTTTTTTTTTTVN, where V is A, C, and G and N are A, C, G, and T. The cDNA of a panel of 33 microRNAs was amplified by RT-qPCR on a LightCycler480. Each 10 μL of reaction contained 3 μL of cDNA, 5 μL of 2X LightCycler 480 SYBR Green I Master (Roche, Germany), 250 nM of each primer (Sigma-Aldrich, Germany), and 1 μL of H_2O. The target miRNAs and the sequences of the primers used for the amplification are listed in the Supplementary Table S2. Cycling conditions were 95 °C for 1 min, followed by 55 cycles of 95 °C for 1 min, and 65 °C for 30 s. Cycle threshold (Ct) values were calculated with the Lightcycler software package and then normalized with *U6* values.

2.10. Anchorage-independent growth ability measurement

The anchorage-independent growth potential of chronically exposed PTP cells to PSNPLs was determined by analyzing the ability to form colonies in a soft-agar medium. Briefly, single-cell suspensions were obtained by filtering cells through a 40 μm mesh. Then, a suspension of 65,000 cells in 1.75 mL of DMEM containing 10 % of FBS and 2.5 μg/mL of Plasmocin was prepared and mixed in a 1:1:1 ratio with 2x DMEM containing 20 % of FBS, 2 % non-essential amino acids, 2 % L-Glu 200 mM, and 2 % penicillin-streptomycin and with 1.2 % of bacto-agar (DIFCO, MD, USA). Dispensing 1.5 mL of the mixture, triplicates of 20,000 cells each were prepared in each well of a 6-well plate over a 0.6 % base agar (supplemented with 2x DMEM). Once the agar was dry, the plates were kept in the incubator for 21 days. Then, the colonies were stained by incubating with 1 mg/mL of (2-p-iodophenyl)− 3–3(p-nitrophenyl)− 5-phenyl tetrazolium chloride (INT; Sigma-Aldrich, Germany). For quantification, the plates were scanned with an HP Scanjet G4050, and the number of colonies was determined using the colony cell counter enumerator software OpenCFU (3.9.0).

2.11. Invasion and migration ability detection

Invasion and migration assays were performed to evaluate the invasive potential of PTP cells long-term exposed to PSNPLs. To that aim, cells at 80 % confluency were deprived of FBS for 24 h. The following day, each 8 μm pore size polycarbonate membrane 24 mm transwell insert (Costar-Corning, NY, USA) was coated with a 180 μL 1:2 dilution of Matrigel® (Costar-Corning, NY, USA) in FBS free DMEM/F12 with 0.1 % BSA. The Matrigel® mixture dried for 1 h in the cell incubator at 37 ºC. After that, 2.5 mL DMEM/F12 complemented with 15 % FBS was added to the bottom chamber of the transwell as the chemo-attractant medium. A single-cell suspension containing 600,000 FBS-deprived MEF cells in 1.5 mL of FBS free DMEM/F12 with 0.1 % BSA was added on top of the transwell Matrigel®-coated membrane. Then, the plates were incubated at 37 ºC for 48 h. To determine the proportion of invading cells, the cell monolayer and Matrigel® mix on top of the transwell were removed with a cotton swab, and the cells adhered to the bottom part of the membrane were fixed with 1 mL methanol (VWR International, Ireland) and stained with 0.2 % crystal violet (Sigma-Aldrich, Germany). After sequential washes, the membranes were allowed to dry and then photographed with a Zeiss Observer A1 microscope. The proportion of migrating or invading cells was measured with ImageJ software.

2.12. Tumorsphere formation ability detection

Exposed and control PTP cells were seeded at a density of 2500 cells/mL on 96-well ultra-low-attachment plates (Corning, Costar-Corning, NY, USA) in serum-free DMEM/F12 supplemented with B27, 20 ng/mL basic fibroblast growth factor (bFGF) (both from Life Technologies, NY, USA), epithelial growth factor, and 4 μg/mL heparin (both from Sigma-Aldrich, Germany). Cells were incubated for 6 days in a humidified atmosphere of 5 % CO_2 and 95 % air at 37 ºC. Then, the observed tumorspheres were counted and photographed using a Zeiss Observer A1 microscope. Tumorspheres' mean size was determined with ImageJ software.

3. Results

3.1. PSNPLs characterization

According to the measurements taken from TEM images (Fig. 1A),

A

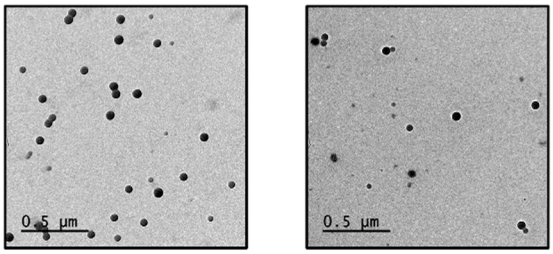

B

	Distilled H_2O	DMEM
Median size (nm) (TEM)	52.99 ± 14.68	48.59 ± 16.38
PdI (DLS)	0.10 ± 0.09	0.44 ± 0.09
Z-potential (mV) (LDV)	-36.00 ± 7.88	-9.31 ± 0.67
Mobility (µm cm/Vs) (LDV)	-2.29 ± 0.10	-0.71 ± 0.05

Fig. 1. : Nanoplastic characterization. (A) Representative TEM images of PSNPLs dispersed in distilled water or DMEM (B) PSNPLs characterization by TEM (median size) and Zetasizer Nano ZS (mean ± SD). Each material was diluted at a concentration of 100 µg/mL for characterization.

PSNPLs are round-shaped particles with equivalent sizes when diluted both in distilled water or in DMEM. The approximate 50 nm diameter measured in our samples agrees with the size indicated by the manufacturer. The nanoplastic particles were further characterized by a Zetasizer device (Fig. 1B). The polydispersity index (PdI) and the Z-potential values indicate that the samples are highly stable monodispersions in water, while they show a propensity to aggregation when diluted in DMEM. The characterization of y-PSNPLs (data not shown) demonstrated that both, the fluorescently labeled and non-labeled nanoplastic, display comparable features, as was previously reported by us (Cortés et al., 2020).

3.2. PSNPLs short-term cytotoxicity, internalization, and cellular localization

PTP cells were exposed for 24 h to increasing doses of PSNPLs (0, 10, 25, 75, and 100 µg/mL), showing low levels of cytotoxicity (Fig. 2A). Although cell viability is over 80 % for all tested doses, we selected 25 µg/mL for the rest of the experimental procedures involving both short- and long-term exposures. This concentration is in the low-dose range and, therefore, appropriate when aiming to recreate realistic exposure conditions.

Despite the lack of cytotoxic effects, results showed a very significant uptake of PSNPLs by the cells. The mean fluorescence intensity was quantified by flow cytometry in living PTP cells exposed to 25 µg/mL y-PSNPLs at 24, 48, and 72 h (Fig. 2B). Our results evidence that nanoplastic uptake reaches its maximum at 48 h, although internalized levels are highly significant at all time points studied when compared to non-exposed cells.

At a cellular level, PSNPLs' localization was further explored by TEM. As seen in Fig. 3, vacuoles loaded with sphere-like particles (indicated with black or white arrows) are found in exposed PTP cells, but not in the control cells. We identified the observed particles as PSNPLs. Interestingly, we consistently found bigger vacuoles after the 48 h of exposure, smaller ones after 72 h, and the smallest ones were observed 24 h after the exposure. This observation agrees with the variations in the fluorescence intensity levels detected by flow cytometry.

3.3. Stress-related gene expression changes

After the sustained 6-month exposure of PTP cells to PSNPLs (25 µg/mL), we evaluated different endpoints related to the oncogenic process. We analyzed the gene expression pattern of stress-related genes, including *Keap*, *Glut-1*, *Gstp-1*, *Nrf2*, *Pgp*, *Sod1,* and *Sod2*. From this gene panel, we could observe that *Gstp-1* was the only upregulated gene, while the expression of *Keap*, *Nrf2*, *Pgp*, *Sod1,* and *Sod2* was significantly downregulated (Fig. 4). Taken together, these results show that stress response is altered by chronic PSNPL exposure which may render the cells more susceptible to oxidative and stress-related damage.

3.4. microRNA expression deregulation

The expression of a battery of 33 microRNAs related to oncogenesis was assessed in chronically exposed PTP cells. Out of the whole set, miR-33a, miR-124, miR-126, miR-132, miR-224, miR-505, miR-541, and miR-544a were not expressed in our system. Among the expressed microRNAs, many presented significant differences in their levels when comparing PSNPL-exposed and non-exposed cells (Fig. 5). Most of these microRNAs were upregulated (miR-21, miR-23a, miR-25, miR-30c, miR-30d, miR-96, miR-135b, miR-148b, miR-155, miR-199b, miR-200a, miR-210, miR-218, and miR-502) while only miR-34a and miR-203a appeared significantly downregulated. Among those overexpressed microRNAs, miR-21, miR-23a, miR-30d, miR-96, miR-210, and miR-502 showed higher expression levels (more than 5 folds of expression compared to control cells).

3.5. Oncogenic phenotype exacerbation

Several biomarkers representative of features developed by the cells over the oncogenic process were studied in PSNPLs long-term exposed PTP cells, to determine if the transformed phenotype of the cells was

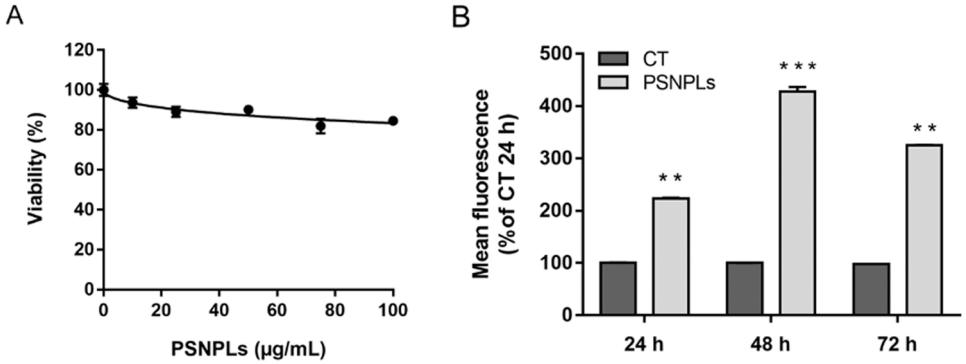

Fig. 2. : Nanoplastic cytotoxicity and internalization in PTP cells. (A) Cell viability of PTP cells exposed to increasing doses of PSNPLs for 24 h. Data are presented as the number of exposed cells relative to the non-exposed control ± SEM (B) y-PSNPLs internalization in PTP cells exposed for 24, 48, or 72 h to 25 µg/mL indicated as mean fluorescence intensity values ± SEM. Statistical significance was determined by one-way ANOVA with Dunnett's post-test (**$P \leq 0.01$; ***$P \leq 0.001$).

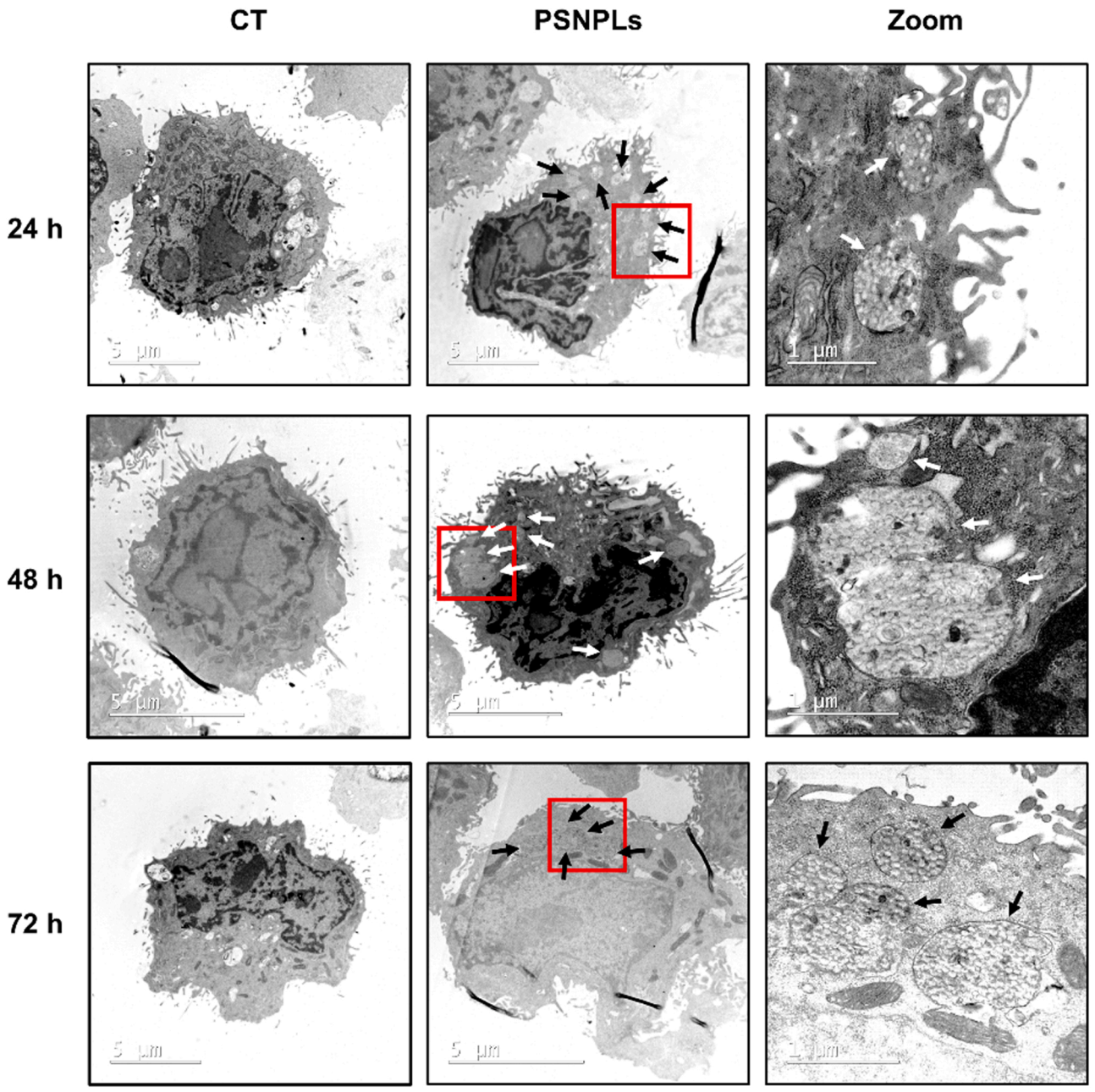

Fig. 3. : Representative TEM images of PTP cells after 24, 48, or 72 h of exposure to 25 µg/mL PSNPLs. Vacuoles loaded with spherical particles are indicated by black and white arrows. The red square indicates the area where the image has been zoomed in.

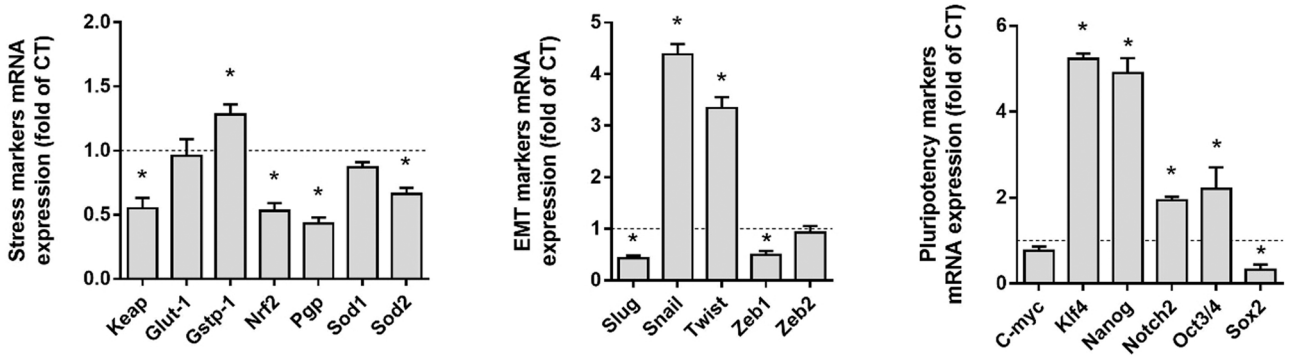

Fig. 4. : Gene expression analysis by RT-qPCR for a panel of stress response-related genes. Data are shown as the fold change of expression in exposed PTP cells compared to non-exposed controls per gene. Values are presented as mean ± SEM for each gene analyzed by the student's t-test (*$P \leq 0.05$).

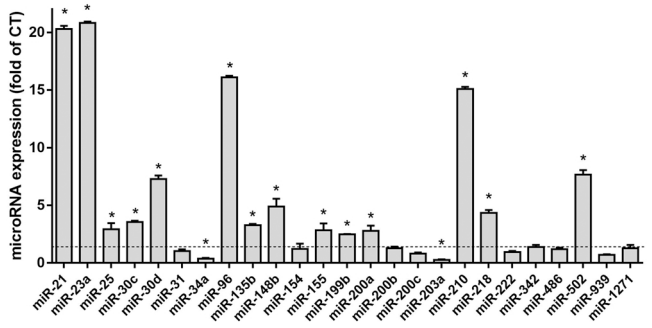

Fig. 5. : Expression analysis for a battery of microRNA by RT-qPCR. Data are plotted as fold changes of PSNPLs-exposed cells' expression compared to controls. Values represent mean ± SEM. Results were analyzed with the student's t-test for each miRNA (* $P < 0.05$).

aggravated by PSNPLs exposure. On the one hand, we evaluated five genes related to EMT and tumor progression to a metastatic phenotype. Interestingly, *Slug* and *Zeb1* expression was downregulated in exposed PTP cells, while *Snail* and *Twist* were overexpressed (Fig. 6 A). Therefore, there are molecular alterations induced by PSNPLs exposure that may eventually lead to EMT deregulation. At a functional level, different endpoints associated with the development of an aggressive tumoral phenotype were explored. Nanoplastic-exposed cells displayed an increased potential to grow independently of anchorage forming colonies in the soft-agar assay (Figs. 6B and 6 C), and presented higher migration (Figs. 6D and 6E), and invasion (Fig. 6 F and 6 G) potentials than control PTP cells. These results indicate that, under chronic exposure settings, PSNPLs induce the development of a significantly aggressive oncogenic phenotype.

3.6. Stemness biomarkers alteration

To further characterize the oncogenic phenotype induced by PSNPLs long-term exposure, several stemness biomarkers were evaluated. As seen in Fig. 7A, the expression analysis of a panel of pluripotent markers showed that exposed PTP cells presented increased levels of *Klf4, Nanog, Notch2,* and *Oct3/4* as well as decreased levels of *Sox2*. Therefore, at a molecular level, stem-related markers are altered by PSNPLs exposure. This deregulation is consistent with the result obtained when the tumorsphere formation ability of PTP cells was determined. The ability of the cells to grow to form tumorspheres is associated with the presence of stem or progenitor cells in tumoral populations. Although no differences in the number of tumorspheres were found, we could observe that PSNPL-exposed cells formed spheres of a significantly bigger diameter than those generated by non-exposed PTP cells. All these results together

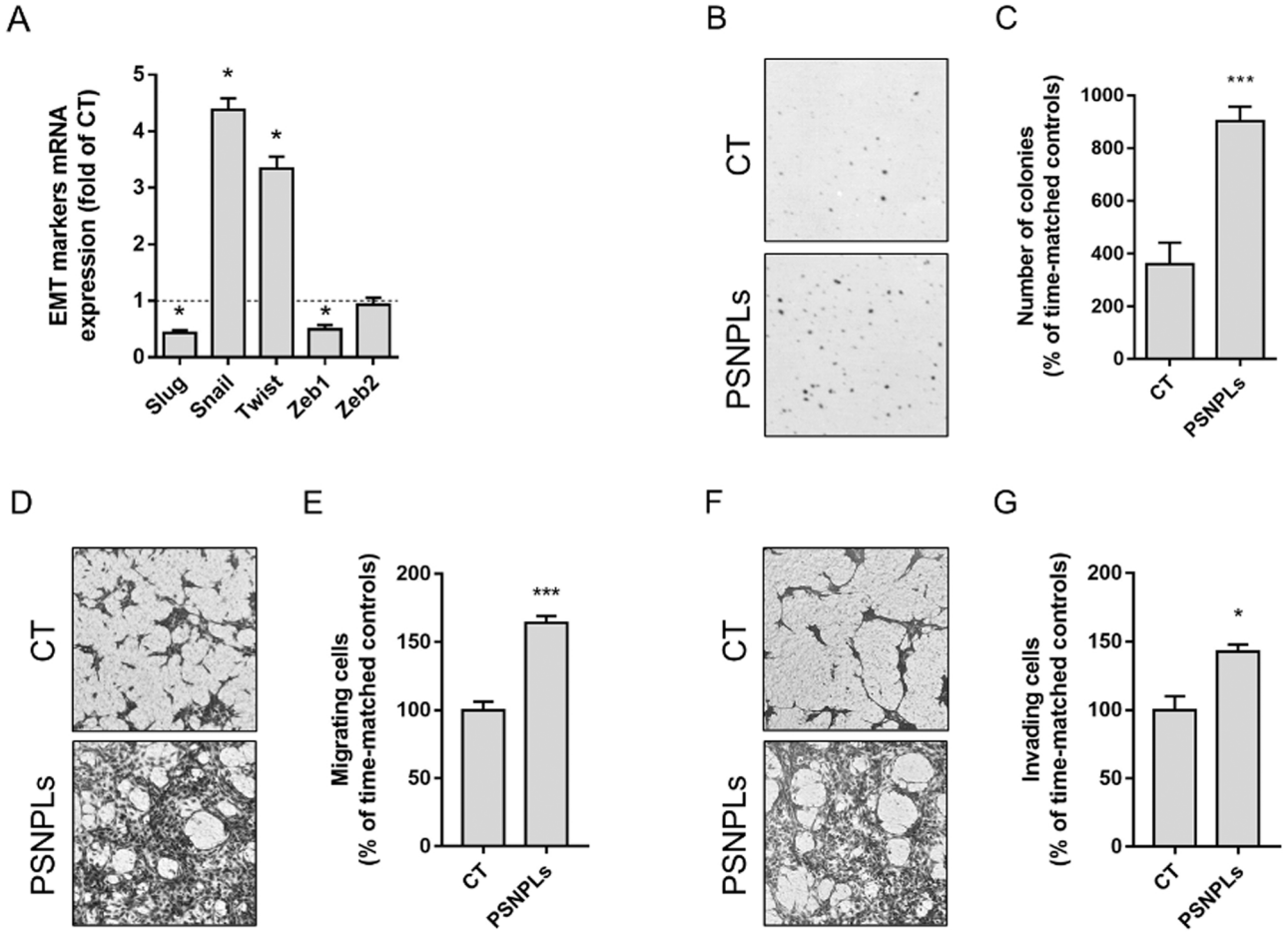

Fig. 6. : Evaluation of the *in vitro* transformed phenotype of PTP cells after the long-term nanoplastic exposure. (A) Expression levels for a set of EMT-related genes. Values are presented as fold changes in exposed cells compared to non-exposed controls. (B) Representative images of colonies growing independently of anchorage in the soft-agar assay. (C) The number of colonies quantified in the soft-agar assay. (D) Representative images of the cells able to translocate to the basal side of the transwell membrane in the migration assay. (E) The proportion of migrating cells is represented as the percentage of exposed cells quantified in the basal part of the membrane compared to controls. (F) Representative images of invading cells observed in the basal side of the transwell membrane. (G) Quantification of the percentage of invading PTP cells after the exposure compared to non-exposed cells. Quantified data are represented as mean ± SEM. Results were analyzed with the student's t-test for each endpoint (* $P < 0.05$; *** $P < 0.001$).

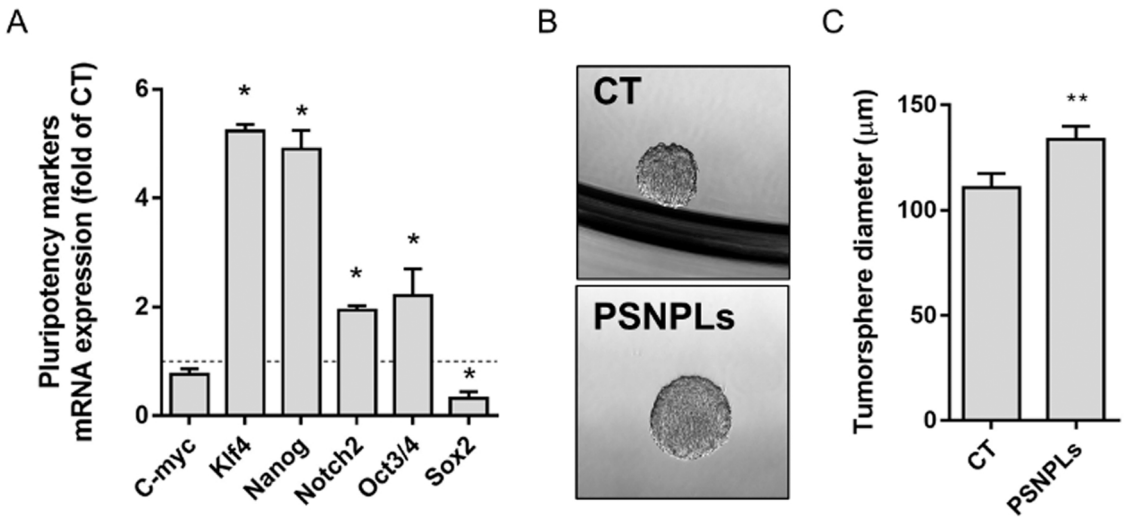

Fig. 7. : Study of stem-related features. (A) Gene expression analysis of a set of pluripotent markers. Values are shown as fold changes in exposed PTP cells compared to non-exposed cells. (B) Representative images of the tumorspheres formed by PSNPL-exposed cells and control cells. (C) Tumorspheres diameter showing the increment in the size of exposed PTP cells -derived tumorspheres. Quantified data are presented as mean ± SEM. Results were analyzed with the student's t-test for each endpoint (* $P < 0.05$; ** $P < 0.01$).

hint at a potential role of PSNPLs in inducing the dedifferentiation of the culture under our exposure conditions.

4. Discussion

The potential health risks associated with human exposure to MNPLs is a hot topic being reviewed in different recent issues (Rubio et al., 2020b; Facciolà et al., 2021; Danopoulos et al., 2021; Das et al., 2021). The lack of powerful enough tools to determine the exposure levels to MNPLs in humans prevents the use of human biomonitoring approaches, as the most direct way to determine the human risks linked to such exposures. In this way, most of the information we have in our hands results from *in vitro* studies using human/mammalian cell lines, although some *in vivo* studies using mammalian models have also been carried out (Yong et al., 2020).

Most of the reported *in vitro* studies lack relevant information, mainly about the exposure type and on the evaluated endpoints, which are useful requirements for their extrapolation to human health risks assessment (Brachner et al., 2020). The most used *in vitro* exposure approaches involve high concentrations and short exposure times, which is far away from the real exposure scenario, where individuals are chronically exposed to low concentrations. Thus, in general, there is a lack of studies using long-term exposure conditions, which better reflect the *in vivo* situation (Yong et al., 2020; Llewellyn et al., 2021). This general criticism also serves for the case of MNPLs, where very few *in vitro* studies using long-term exposures have been published until now (Visalli et al., 2021; Domenech et al., 2021; Gopinath et al., 2021). In this context, our study with exposures lasting for 6 months must be highlighted for its novelty and effort to simulate a more realistic exposure scenario. It should be mentioned that, although this type of experimental approach involves a time/economic consuming design, this type of long-term exposure scenario is very relevant to identifying potential hazards affecting human health. It is easy to understand that, faced with the experimental complexity indicated above, many researchers avoid it. However, if we agree with its usefulness and relevance, efforts using long-term approaches must be done.

Regarding the potential health effects associated with MNPLs exposure, the carcinogenic risk stands up. Although the standard way to determine the carcinogenic risk of any agent implies the use of lab mammals (OECD, 2018), the risk assessment of potential carcinogens has evolved from simply counting tumors present in animals to long-term bioassays to understanding the mechanistic basis for chemical-induced cancers (Bhat et al., 2020). Using such new approaches, plausible modes of action (MOA) for environmental agents, mainly for emergent pollutants such as MNPLs, can be determined using *in vitro* experiments. Considering that tumor induction is a multistep process requiring prolonged exposures, long-term experimental approaches, such those used in this study, are needed to go deeper into the determination of the potential carcinogenic risk of MNPLs exposure.

Interestingly, our results clearly show that many of the used biomarkers of our battery of cancer hallmarks are exacerbated after long-term exposure to MNPLs. Such cancer hallmarks constitute a reference framework, summarizing the abilities of cancer cells to escape control (Hanahan and Weinberg, 2011). At this point, we wish to highlight the usefulness of our PTP cell model, highly sensitive to the action of agents with tumorigenic potential, and the use of concurrent controls to identify if observed changes could be associated with the long-term growing conditions. MEF cells, knockdown for different genes, have shown their usefulness to discover mechanisms involved in oncogenesis. This occurs with *FRA1,* a transcription factor frequently overexpressed in epithelial tumors, playing an essential role in the *in vitro* cell transformation induced by arsenic (Barguilla et al., 2020); or with the *Atg5* (autophagy-related gene 5) knockdown, playing a role on the levels of inflammation-related proteins and apoptosis induced by polystyrene nanoplastics (Wang et al., 2021). In the present study, PTP cells have been shown to dramatically accumulate large amounts of polystyrene nanoplastics, mainly after exposures lasting for 48 h. This easy uptake reaffirms the usefulness of our selected cell model to evaluate the effects of MNPLs.

As previously mentioned, the more relevant finding of our study is that most of the used hallmarks of cancer are exacerbated, independently if they are associated with an early tumoral phenotype (changes in stress-related genes or microRNA deregulation), advanced tumoral phenotype (growing independently of anchorage ability and migration capacity), or an aggressive tumoral phenotype (invasion ability, changes in pluripotency markers, and ability to grow to form tumorspheres). All this information constitutes a relevant warning on the potential carcinogenic risk associated with long-term exposures to MNPLs, at least regarding the PSNPLs evaluated in this study. Despite the lack of studies aiming to directly determine the carcinogenicity of MNPLs some studies have determined adverse outcome pathways (AOP) associated with their exposures. Thus, using *Daphnia*, a proposed AOP for polystyrene

nanoplastics included ROS production and oxidative stress as the molecular initiating events, followed by changes in specific signaling and metabolism pathways. These processes lead to effects such as growth inhibition and altered reproductive outputs (Liu et al., 2021a).

In our study, changes in the expression levels of different EMT markers (*Slug, Snail, Twist, Zeb*) have been found associated with long-term exposure to PSNPLs. The mesenchymal phenotype is closely associated with malignant transformation and linked to the migration phenotype. Although no previous studies are using MNPLs, such changes have been reported to occur associated with exposure to different plasticizers such as bisphenol A and phthalates (Lee et al., 2017). Interestingly, changes in cell migration ability were also observed in human umbilical vein endothelial cells exposed to polystyrene microplastics, together with the inhibition of angiogenic tube formation, suppression of angiogenic signaling pathways, and inhibitory activity against wound healing (Lee et al., 2021).

microRNAs usually act post-transcriptionally to suppress the expression of many targeted genes, and different studies have demonstrated that they are crucial players in numerous biological processes such as inflammation, proliferation, differentiation, development, and apoptosis, among others (Chekhun, 2019). In the used battery of microRNAs, related to cell transformation processes, we have found a large impact on miRNA expression profiling after our long-term exposure to PSNPLs. Interestingly, the expression of mir-21, mir 23a, mir-96, and mir-210 was also altered in BEAS-2B cells exposed to cigarette smoke condensate (Ballesteros et al., 2021a) and zinc-oxide and titanium dioxide nanoparticles (Ballesteros et al., 2021b), agents able to produce cell transformation in a long-term exposure scenario. These two studies used the same battery of microRNAs associated with cell transformation processes that have been used in the present study. Interestingly, *in vivo* dysregulation of different microRNAs has been observed in *Caenorhabditis elegans* exposed to polystyrene nanoparticles, and has been associated with various biological processes and signaling pathways (Qu et al., 2019). Moreover, these dysregulated microRNAs were observed to be involved in the resistance to the toxicity of polystyrene nanoparticles. Using this *in vivo* model, the overexpression of mir-35 was also observed (Li et al., 2020), and it is worth recalling that this microRNA was also upregulated in our study. In the intestine of *C. elegans*, NDK-1 was identified as the direct target of mir-35, and the kinase suppressors of Ras (KSR-1 and KSR-2) were further identified as downstream targets of intestinal NDK-1. This information would support the view indicating a tumoral risk associated with PSNPLs. More interestingly, and to confirm the goodness of our results, three others of the microRNA dysregulated in our study (mi-794, mi-38, and mi-76) have also been found dysregulated in *C. elegans* exposed to nanopolystyrene (Qiu et al., 2020; Yang et al., 2020; Liu et al., 2021b). All this reinforces the usefulness of the used microRNAs battery to pick up those micro-RNAs responding to the long-term exposure to MNPLs.

Our results also show that PSNPLs exposure targeted stem cells. This is reflected by the altered expression of different pluripotent markers such as *Klf4, Nanog, Notch2, Oct3/4,* and *Sox2* genes which play a dominant role in regulating pluripotency (Hadjimichael et al., 2015). No other studies have used such biomarkers to unravel the mechanisms involved in MNPLs exposure. Furthermore, such long-term exposure was able to increase the size of the induced tumorspheres, which are associated with the presence of stem-like cells in the cell population. Tumorsphere analysis is widely used to analyze the self-renewal capability of cancer stem cells and to detect both pro-tumoral and anti-tumoral agents/effects (Lee et al., 2016). An alternative way to evaluate the effects on stem cells is the use of mini-organoid cultures obtained from various types of stem cells. Such *ex vivo* models are promising tools for a more comprehensive understanding of the underlying mechanisms involved in *in vitro* toxicities (Bredeck et al., 2022). Interestingly, a very recent study has evaluated the effects of PSMPLs on liver organoids generated from human pluripotent stem cells, as an alternative model to the human liver. Using that model, the authors observed an increased expression of hepatic HNF4A and CYP2E1. Accordingly, an AOP relevant to PSMPLs was proposed, where their potential risks of liver steatosis, fibrosis, and cancer were implicated (Cheng et al., 2022). These results would confirm our findings pointing out the potential carcinogenic risk of long-term PSNPs exposures.

In addition to the potential direct carcinogenic effects of MNPLs, many studies point out the potential synergies between MNPLs and carcinogenic pollutants. The adsorption of carcinogenic polycyclic aromatic hydrocarbons (PHA) onto microplastics has been proposed as a potential mechanism to increase the probable cancer risk of ingested PAHs-enriched MNPLs (Sharma et al., 2020). Similarly, the co-exposure of tetracycline and polystyrene nanoplastics also exacerbates different biomarkers in juvenile grass carp. The authors described enhanced oxidative damage under co-exposure conditions, as well as increased expression levels of MMP2, MMP9, and IL-8 both in liver and intestine tissues. Since mRNA expression of MMP2 is positively correlated with TGFβ1, IL8, and MMP9 in liver hepatocellular carcinoma and colon adenocarcinoma, that study points out an increased cancer risk associated with such co-exposure (Liu et al., 2022).

In conclusion, our results add relevant information supporting a potential carcinogenic risk associated with MNPLs exposure, when long-term exposures take place. Due to the relevance of these findings, further experimental approaches are required to decipher the link between MNPLs exposure and cancer risk.

Environmental implication

Environmental carcinogenesis is an old topic but updated according the presence of new emergent environmental contaminants, such as micro/nanoplastics. For such pollutants, is urgent to determine their potential carcinogenic risk. Due to the lack of information on this topic, and to avoid the use of experimental mammals, we have designed a battery of in vitro approaches containing different cancer hallmarks. Interestingly, our approach using nanopolystyrene as a model and a long term (6 months) exposure demonstrate exacerbated tumoral phenotypes after exposure. Our data constitutes a relevant warning on the potential carcinogenic risk associated with long-term exposures to MNPLs.

CRediT authorship contribution statement

RM and AH planned the experiments. IB, SB, JD, and LR carried out the experimental part. IB analyzed the data, carried out the statistical analysis, and prepared tables/figures. IB, RM, and AH wrote the final manuscript.

Declaration of Competing Interest

The authors declare that they have no known competing financial interests or personal relationships that could have appeared to influence the work reported in this paper.

Data Availability

Data will be made available on request.

Acknowledgments

We wish to thank Mr. C. Valiente for his technical assistance. The authors I. Barguilla S. Ballesteros, and J. Domenech were supported by PhD fellowships from the Universitat Autònoma de Barcelona [PIF-UAB]. L. Rubio was supported by the Fondo Nacional de Innovación y Desarrollo Científico y Tecnológico (FONDOCYT) República Dominicana (Project 2018-2019-2B2-093). This work was partially supported by the Spanish Ministry of Science and Innovation [PID2020-116789, RB-C43]. This project has received funding from the European Union's Horizon 2020 research and innovation programme under grant

agreement No 965196 (PlasticHeal).

Author contribution statement

RM and AH planned the experiments. IB, SB, JD, and LR carried out the experimental part. IB analyzed the data, carried out the statistical analysis, and prepared tables/figures. IB, RM, and AH wrote the final manuscript.

Appendix A. Supporting information

Supplementary data associated with this article can be found in the online version at doi:10.1016/j.jhazmat.2022.129470.

References

Annangi, B., Bach, J., Vales, G., Rubio, L., Marcos, R., Hernández, A., 2015. Long-term exposures to low doses of cobalt nanoparticles induce cell transformation enhanced by oxidative damage. Nanotoxicology 9 (2), 138–147. https://doi.org/10.3109/17435390.2014.900582.

Bach, J., Peremartí, J., Annangi, B., Marcos, R., Hernández, A., 2016. Oxidative DNA damage enhances the carcinogenic potential of *in vitro* chronic arsenic exposures. Arch. Toxicol. 90 (8), 1893–1905. https://doi.org/10.1007/s00204-015-1605-7.

Ballesteros, S., Domenech, J., Barguilla, I., Cortés, C., Marcos, R., Hernández, A., 2020. Genotoxic and immunomodulatory effects in human white blood cells after *ex vivo* exposure to polystyrene nanoplastics. Environ. Sci. Nano 7, 3431–3446. https://doi.org/10.1039/D0EN00748J.

Ballesteros, S., Barguilla, I., Marcos, R., Hernández, A., 2021a. Nanoceria, alone or in combination with cigarette-smoke condensate, induce transforming and epigenetic cancer-like features *in vitro*. Nanomedicine 16 (4), 293–305. https://doi.org/10.2217/nnm-2020-0367.

Ballesteros, S., Vales, G., Velázquez, A., Pastor, S., Alaraby, M., Marcos, R., Hernández, A., 2021b. microRNAs as a suitable biomarker to detect the effects of long-term exposures to nanomaterials. Studies on TiO_2NPs and MWCNTs. Nanomaterials 11, 3458. https://doi.org/10.3390/nano11123458.

Bhat, V.S., Cohen, S.M., Gordon, E.B., Wood, C.E., Cullen, J.M., Harris, M.A., Proctor, D. M., Thompson, C.M., 2020. An adverse outcome pathway for small intestinal tumors in mice involving chronic cytotoxicity and regenerative hyperplasia: a case study with hexavalent chromium, captan, and folpet. Crit. Rev. Toxicol. 50 (8), 685–706. https://doi.org/10.1080/10408444.2020.1823934.

Barguilla, I., Bach, J., Peremartí, J., Marcos, R., Hernández, A., 2020. FRA1 is essential for the maintenance of the oncogenic phenotype induced by in vitro long-term arsenic exposure. Metallomics 12 (12), 2161–2173. https://doi.org/10.1039/d0mt00209g.

Bouwmeester, H., Hollman, P.C., Peters, R.J., 2015. Potential health impact of environmentally released micro- and nanoplastics in the human food production chain: experiences from nanotoxicology. Environ. Sci. Technol. 49 (15), 8932–8947. https://doi.org/10.1021/acs.est.5b01090.

Brachner, A., Fragouli, D., Duarte, I.F., Farias, P.M.A., Dembski, S., Ghosh, M., Barisic, I., Zdzieblo, D., Vanoirbeek, J., Schwabl, P., Neuhaus, W., 2020. Assessment of human health risks posed by nano-and microplastics is currently not feasible. Int J. Environ. Res. Public Health 17 (23), 8832. https://doi.org/10.3390/ijerph17238832.

Bredeck, G., Halamoda-Kenzaoui, B., Bogni, A., Lipsa, D., Bremer-Hoffmann, S., 2022. Tiered testing of micro- and nanoplastics using intestinal in vitro models to support hazard assessments. Environ. Int. 158, 106921 https://doi.org/10.1016/j.envint.2021.106921.

Chekhun, V.F., 2019. MicroRNAs are a key factor in the globalization of tumor-host relationships. Exp. Oncol. 41, 188–194. https://doi.org/10.32471/exp-oncology.2312-8852.vol-41-no-3.13431.

Cheng, W., Li, X., Zhou, Y., Yu, H., Xie, Y., Guo, H., Wang, H., Li, Y., Feng, Y., Wang, Y., 2022. Polystyrene microplastics induce hepatotoxicity and disrupt lipid metabolism in the liver organoids. Sci. Total Environ. 806 (Pt1), 150328 https://doi.org/10.1016/j.scitotenv.2021.150328.

Cortés, C., Domenech, J., Salazar, M., Pastor, S., Marcos, R., Hernández, A., 2020. Nanoplastics as potential environmental health factors. Effects of polystyrene nanoparticles on the human intestinal epithelial Caco-2 cells. Environ. Sci. Nano 7, 272–285. https://doi.org/10.1039/c9en00523d.

Danopoulos, E., Twiddy, M., West, R., Rotchell, J.M., 2021. A rapid review and meta-regression analyses of the toxicological impacts of microplastic exposure in human cells. J. Hazard Mater. 24, 127861 https://doi.org/10.1016/j.jhazmat.2021.127861.

Das, R.K., Sanyal, D., Kumar, P., Pulicharla, R., Brar, S.K., 2021. Science-society-policy interface for microplastic and nanoplastic: environmental and biomedical aspects. Environ. Pollut. 290, 117985 https://doi.org/10.1016/j.envpol.2021.117985.

Domenech, J., Hernández, A., Rubio, L., Marcos, R., Cortés, C., 2020. Interactions of polystyrene nanoplastics with *in vitro* models of the human intestinal barrier. Arch. Toxicol. 94 (9), 2997–3012. https://doi.org/10.1007/s00204-020-02805-3.

Domenech, J., de Britto, M., Velázquez, A., Pastor, S., Hernández, A., Marcos, R., Cortés, C., 2021. Long-term effects of polystyrene nanoplastics in human intestinal Caco-2 cells. Biomolecules 11, 1442. https://doi.org/10.3390/biom11101442.

Domenech, J., Marcos, R., 2021. Pathways of human exposure to microplastics, and estimation of the total burden. Curr. Opin. Food Sci. 39, 144–151. https://doi.org/10.1016/j.cofs.2021.01.004.

Facciolà, A., Visalli, G., Pruiti Ciarello, M., Di Pietro, A., 2021. Newly emerging airborne pollutants: current knowledge of health impact of micro and nanoplastics. Int J. Environ. Res. Public Health 18 (6), 2997. https://doi.org/10.3390/ijerph18062997.

Gopinath, P.M., Twayana, K.S., Ravanan, P., Thomas, John, Mukherjee, A., Jenkins, D.F., Chandrasekaran, N., 2021. Prospects on the nano-plastic particles internalization and induction of cellular response in human keratinocytes. Part Fibre Toxicol. 18 (1), 35. https://doi.org/10.1186/s12989-021-00428-9.

Hadjimichael, C., Chanoumidou, K., Papadopoulou, N., Arampatzi, P., Papamatheakis, J., Kretsovali, A., 2015. Common stemness regulators of embryonic and cancer stem cells. World J. Stem Cells 7, 1150–1184. https://doi.org/10.4252/wjsc.v7.i9.1150.

Hanahan, D., Weinberg, R.A., 2011. Hallmarks of cancer: the next generation. Cell 144 (5), 646–674. https://doi.org/10.1016/j.cell.2011.02.013.

Hesler, M., Aengenheister, L., Ellinger, B., Drexel, R., Straskraba, S., Jost, C., Wagner, S., Meier, F., von Briesen, H., Büchel, C., Wick, P., Buerki-Thurnherr, T., Kohl, Y., 2019. Multi-endpoint toxicological assessment of polystyrene nano- and microparticles in different biological models in vitro. Toxicol. Vitr. 61, 104610 https://doi.org/10.1016/j.tiv.2019.104610.

Hu, M., Palić, D., 2020. Micro- and nano-plastics activation of oxidative and inflammatory adverse outcome pathways. Redox Biol. 37, 101620 https://doi.org/10.1016/j.redox.2020.101620.

Lee, C.H., Yu, C.C., Wang, B.Y., Chang, W.W., 2016. Tumorsphere as an effective *in vitro* platform for screening anti-cancer stem cell drugs. Oncotarget 7 (2), 1215–1226. https://doi.org/10.18632/oncotarget.6261.

Lee, H.M., Hwang, K.A., Choi, K.C., 2017. Diverse pathways of epithelial mesenchymal transition related with cancer progression and metastasis and potential effects of endocrine disrupting chemicals on epithelial mesenchymal transition process. Mol. Cell Endocrinol. 457, 103–113. https://doi.org/10.1016/j.mce.2016.12.026.

Lee, H.S., Amarakoon, D., Wei, C.I., Choi, K.Y., Smolensky, D., Lee, S.H., 2021. Adverse effect of polystyrene microplastics (PS-MPs) on tube formation and viability of human umbilical vein endothelial cells. Food Chem. Toxicol. 154, 112356 https://doi.org/10.1016/j.fct.2021.112356.

Li, D., Yuan, Y., Wang, D., 2020. Regulation of response to nanopolystyrene by intestinal microRNA mir-35 in nematode *Caenorhabditis elegans*. Sci. Total Environ. 736, 139677 https://doi.org/10.1016/j.scitotenv.2020.139677.

Liu, Z., Li, Y., Sepúlveda, M.S., Jiang, Q., Jiao, Y., Chen, Q., Huang, Y., Tian, J., Zhao, Y., 2021a. Development of an adverse outcome pathway for nanoplastic toxicity in *Daphnia pulex* using proteomics. Sci. Total Environ. 766, 144249 https://doi.org/10.1016/j.scitotenv.2020.144249.

Liu, H., Zhao, Y., Bi, K., Rui, Q., Wang, D., 2021b. Dysregulated mir-76 mediated a protective response to nanopolystyrene by modulating heme homeostasis related molecular signaling in nematode *Caenorhabditis elegans*. Ecotoxicol. Environ. Saf. 212, 112018 https://doi.org/10.1016/j.ecoenv.2021.112018.

Liu, S., Yan, L., Zhang, Y., Junaid, M., Wang, J., 2022. Polystyrene nanoplastics exacerbated the ecotoxicological and potential carcinogenic effects of tetracycline in juvenile grass carp (*Ctenopharyngodon idella*). Sci. Total Environ. 803, 150027 https://doi.org/10.1016/j.scitotenv.2021.150027.

Llewellyn, S.V., Niemeijer, M., Nymark, P., Moné, M.J., van de Water, B., Conway, G.E., Jenkins, G.J.S., Doak, S.H., 2021. *In vitro* three-dimensional liver models for nanomaterial DNA damage assessment. Small 17 (15), e2006055. https://doi.org/10.1002/smll.202006055.

OECD. Test No. 451: Carcinogenicity Studies, OECD Guidelines for the Testing of Chemicals, Section 4, OECD Publishing, Paris, 2018. doi: 10.1787/9789264071186-en.

Qiu, Y., Liu, Y., Li, Y., Wang, D., 2020. Intestinal mir-794 responds to nanopolystyrene by linking insulin and p38 MAPK signaling pathways in nematode *Caenorhabditis elegans*. Ecotoxicol. Environ. Saf. 201, 110857 https://doi.org/10.1016/j.ecoenv.2020.110857.

Qu, M., Luo, L., Yang, Y., Kong, Y., Wang, D., 2019. Nanopolystyrene-induced microRNAs response in *Caenorhabditis elegans* after long-term and lose-dose exposure. Sci. Total Environ. 697, 134131 https://doi.org/10.1016/j.scitotenv.2019.134131.

Rubio, L., Barguilla, I., Domenech, J., Marcos, R., Hernández, A., 2020a. Biological effects, including oxidative stress and genotoxic damage, of polystyrene nanoparticles in different human hematopoietic cell lines. J. Hazard Mater. 398, 122900 https://doi.org/10.1016/j.jhazmat.2020.122900.

Rubio L., Marcos R., Hernández A. Potential adverse health effects of ingested micro- and nanoplastics on humans. Lessons learned from in vivo and in vitro mammalian systems. J Toxicol Environ Health PB, 2020b, 23(2): 51–68. doi: 10.1080/10937404.2019.1700598.

Schirinzi, G.F., Pérez-Pomeda, I., Sanchís, J., Rossini, C., Farré, M., Barceló, D., 2017. Cytotoxic effects of commonly used nanomaterials and microplastics on cerebral and epithelial human cells. Environ. Res. 159, 579–587. https://doi.org/10.1016/j.envres.2017.08.043.

Sharma, M.D., Elanjickal, A.I., Mankar, J.S., Krupadam, R.J., 2020. Assessment of cancer risk of microplastics enriched with polycyclic aromatic hydrocarbons. J. Hazard Mater. 398, 122994 https://doi.org/10.1016/j.jhazmat.2020.122994.

Visalli, G., Facciolà, A., Pruiti Ciarello, M., De Marco, G., Maisano, M., Di Pietro, A., 2021. Acute and sub-chronic effects of microplastics (3 and 10 μm) on the human intestinal cells HT-29. Int J. Environ. Res. Public Health 18 (11), 5833. https://doi.org/10.3390/ijerph18115833.

Wang, Y.L., Lee, Y.H., Hsu, Y.H., Chiu, I.J., Huang, C.C., Huang, C.C., Chia, Z.C., Lee, C. P., Lin, Y.F., Chiu, H.W., 2021. The kidney-related effects of polystyrene microplastics on human kidney proximal tubular epithelial cells HK-2 and male C57BL/6 mice. Environ. Health Perspect. 129 (5), 57003. https://doi.org/10.1289/EHP7612.

Yang, Y., Wu, Q., Wang, D., 2020. Epigenetic response to nanopolystyrene in germline of nematode *Caenorhabditis elegans*. Ecotoxicol. Environ. Saf. 206, 111404 https://doi.org/10.1016/j.ecoenv.2020.111404.

Yong, C.Q.Y., Valiyaveettil, S., Tang, B.L., 2020. Toxicity of microplastics and nanoplastics in mammalian systems. Int. J. Environ. Res. Public Health 17 (5), 1509. https://doi.org/10.3390/ijerph17051509.